Analysis of Boundary Layer and Solute Transport in Osmotic Evaporation

J. Romero, G. M. Rios, and J. Sanchez
Institut Européen des Membranes, UM2, CC 047 Pl. Eugène Bataillon, 34090 Montpellier, Cedex 5, France

A. Saavedra
Dept. Ingeniería Química, University Santiago de Chile, Ave. Bdo. O'Higgins 3363, Santiago, Chile

The osmotic evaporation process (OE) is based on the transfer of solvent from a dilute solution to be concentrated to an extraction medium (for example, a highly concentrated brine) separated by a macroporous hydrophobic membrane. Mass transfer takes place in the gas phase through the membrane pores under the influence of the water activity gradient. The OE process has been analyzed before in experiments by Courel et al. in 2000 and models by Romero et al. in 2001. These previous studies take into account the effect of structural membrane parameters and working conditions of water flux performance. An algorithm has been developed to solve the system constituted of the mass- and heat-transfer equations. In order to validate it more easily, the simulation was conducted for the results of pure water evaporation. This provides a lot of interesting information on transfer resistances, temperature, and concentration profiles, as well as the prediction of water flows. A work that is the logical continuation of these previous studies is proposed. First, it aims at explaining the influence of the concentration polarization that develops at the solution–membrane interface when the concentration is applied to a sucrose solution. The transfer of very dilute volatile compounds from the sweetened solution is also analyzed with a view to understanding the mechanism that controls the loss of aroma compounds during the concentration of fruit juices.

Introduction

Membrane technologies working at low temperature, and especially the so-called new "membrane contactors," are very promising processes for fruit juice concentration. In fact, the organoleptic properties as well as flavors of fresh juices are better preserved this way than with classic thermal evaporation. These new techniques are becoming an important subject of research and development even if traditional ones may be slightly more economical in some concentration ranges (Courel et al., 2000b; Bandini and Sarti, 2002; Courel, 1999; Gostoli, 1999).

Several membrane contactor and other technologies have been applied to the concentration of fruit and vegetable juices: osmotic evaporation, membrane distillation, and so on. However, the analysis and explanation of experimental results was frequently made difficult because of the complexity of real solutions. Mass transfer of volatile aroma compounds has been approached by several authors using model solutions that involved just a few well-known species (Courel, 1999; Shaban, 1996; Baudot et al., 1999; Börjesson et al., 1996; Couffin et al., 1998). But no general characterization of transport phenomena has been proposed yet. Based on previous results obtained in our group, this article constitutes a first attempt to explain the mechanisms that control the transfer of a volatile solute from the dilute solution to the extraction brine.

Correspondence concerning this article should be addressed to. G. M. Rios.
Additional address for J. Romero: Dept. Ing. Química, University of Santiago de Chile, Ave. Bdo. O'Higgins 3363, Santiago, Chile.

The main driving force acting on water in osmotic evaporation (OE) is the transmembrane vapor-pressure difference. A quantitative description of simultaneous mass and heat transfer accounting for hydrodynamics and structural membrane characteristics has already been proposed (Romero et al., 2003). In the present study, these results are used to calculate the driving force at interfaces, as well as the resulting convective flux of solvent through the pores.

Another very important phenomenon to be considered in the process is the concentration polarization that could develop along the membrane, especially on the side of the solution to be treated. Indeed, solutions such as fruit juices generally present a high sugar content (sucrose, fructose, glucose, and so on) and their viscosity may increase considerably, thus inducing a strong variation in the concentration at the wall. This is thought to affect the value of the diffusion coefficient in the boundary layer and, thus, the solvent flux. The effect has been highlighted experimentally by Courel and coworkers (Courel et al., 2000a; Courel, 1999). In this work it is fully explained by widening the applicability of the model already presented by our group (Romero et al., 2003).

Finally, it may be easily understood that in the presence of a volatile compound, the selectivity of the process defined as the ratio of the mass of the volatile solute to the mass of the water evaporated, will be closely related to the vapor–liquid equilibrium of the solute considered. More precisely, the knowledge of the volatility of the solute compared to that of water will be essential. Starting with general transport equations, we propose a description of the movement of a very dilute solute representative of an aroma compound, from the sweetened solution where it is located at the initial state, toward the brine used to ensure water extraction. This analysis is completed by considering the thermodynamic characteristics of different species. Then the indications and trends thus obtained are matched with the experimental results obtained by Courel with model solutions representative of the passion fruit (*Passiflora edulis*) juice.

Sugar Boundary-Layered Characteristics

In this first part of the study the presence of very dilute organic compounds is ignored and the only solute that is considered on the solution side is sugar.

Mass-transfer equations

In a previous work (Romero et al., 2003), which was focused on the evaporation of pure water, a model involving only three resistances in-series was considered. These resistances correspond to the hydrophobic porous layer filled with gas, to the macroporous support filled with stagnant liquid, and to the boundary layer on the side of the extraction brine, respectively. In the present study, the concentration boundary layer that is formed on the other side of the membrane when a sweetened solution is treated has been also taken into account. The four different layers considered here for modeling purposes are shown in Figure 1.

Through the polarization layer, the water flow can be expressed as

$$N_w = k_w^{(\mathrm{I})}\left(x_{wf}^b - x_{wf}^m\right) \tag{1}$$

where $k_w^{(\mathrm{I})}$ is the mass-transfer coefficient for water at average conditions in the boundary layer.

As already explained, two mechanisms are possible for the water vapor transport within the pores of the hydrophobic layer: Knudsen and molecular diffusion. The permeances that correspond to these two regimes are given by the following equations

$$G_{Kn}^{(\mathrm{II})} = -\frac{N_w}{\Delta p_w} = \frac{N_w}{p_{wf} - p_{wp}} = \frac{2}{3}\frac{\epsilon_{hl} r_{hl}}{\tau_{hl} L_{hl}}\left[\frac{8}{\pi RTM_w}\right]^{0.5} \tag{2}$$

$$G_{MD}^{(\mathrm{II})} = -\frac{N_w}{\Delta p_w} = \frac{P}{RT}\frac{\epsilon_{hl}}{\tau_{hl}}\frac{D_{wa}}{L_{hl}}\frac{1}{p_{wf} - p_{wp}}\ln\left(\frac{P - p_{wp}}{P - p_{wf}}\right) \tag{3}$$

where r_{hl}, ϵ_{hl}, and τ_{hl} are, respectively, the average pore radius, the porosity, and the tortuosity of the hydrophobic layer; M_w is the molecular weight of water, and D_{wa} represents the diffusion coefficient of the water vapor in the air retained within the pores. In our previous study (Romero et al., 2003) we found that it was not possible to make a distinction between Knudsen-like and molecular diffusion mechanisms, because the water vapor fluxes calculated from both equations are nearly the same. The simulations carried out hereinafter consider the transport of water vapor as a Knudsen-like diffusion.

Ordinarily, it is admitted that the thickness of the gas gap within the pores of the hydrophobic layer is equal to the membrane thickness, L_{hl}. Romero and coworkers (Romero et al., 2003) drew attention to the fact that this assumption has strong implications in that the main resistance is often attached to the gas film. Thus, even weak penetration of the liquid inside the membrane porosity could give a significant variation of the overall mass-transfer resistance by reducing the volume occupied by the entrapped gas.

In the previous publication we found that the extraction brine wets the membrane support and also partially wets the hydrophobic layer. Because the structural characteristics (porosity and tortuosity) of both layers are similar (Romero et al., 2003) we considered only one equation to be at steady state for the mass transport by molecular diffusion through

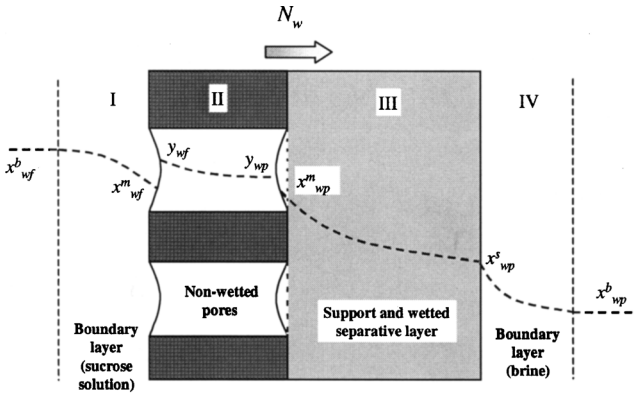

Figure 1. Outline of water mass transfer: concentration profile in the different layers of the system.

the wetted thickness

$$N_w = \frac{\rho_{\text{brine}}^{\text{sup}}}{M_{\text{brine}}^{\text{sup}}} \frac{\epsilon_s}{\tau_s} \frac{D_{wCaCl2}^{(\text{III})}}{L_s} \ln\left(\frac{1-x_{wp}^{s}}{1-x_{wp}^{m}}\right) \quad (4)$$

The density and the molecular weight of the brine, $\rho_{\text{brine}}^{\text{sup}}$ and $M_{\text{brine}}^{\text{sup}}$, are calculated at average conditions.

Finally, the water flow through the brine boundary layer is given by Eq. 5

$$N_w = k_w^{(\text{IV})}\left(x_{wp}^{s} - x_{wp}^{b}\right) \quad (5)$$

Water vapor–liquid equilibrium

The water vapor–liquid equilibrium at the interfaces with the hydrophobic layer is evaluated through the water activity. The UNIFAC method was applied (Achard et al., 1992) to estimate this value on the side of the concentrated sucrose solution. The estimation of the water activity in the concentrated brine was carried out using the modified ASOG group contribution method (Correa et al., 1997). The modified ASOG method is a combination of the UNIFAC method and parts of the Debye-Hückel theory. Two subroutines were introduced into the general program. They enable calculation of the water activity as a function of the sucrose and brine concentration, respectively.

With these methods, the water activity coefficients at interfaces were calculated using two terms: a combinatorial term ($\ln \gamma_i^C$), which considers the shape and size of each group, and a residual term ($\ln \gamma_i^R$), which considers the steric interactions between all the groups present in the liquids. A third term ($\ln \gamma_i^{D\text{-}H}$), which takes the effect of electrostatic interactions into account, was considered for the hypertonic solution (brine). If all long-range interactions of the Debye-Hückel type are considered, the three contributions could be added, leading to

$$\ln \gamma_i = \ln \gamma_i^C + \ln \gamma_i^R + \ln \gamma_i^{D\text{-}H} \quad (6)$$

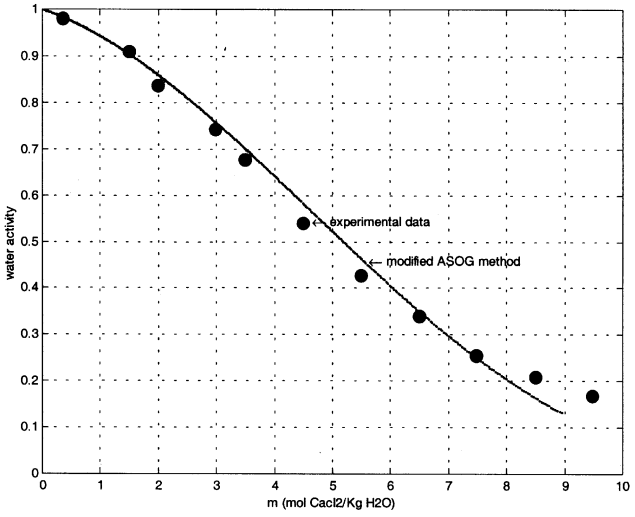

Figure 2. Water activity in a solution of $CaCl_2$ at 298 K.

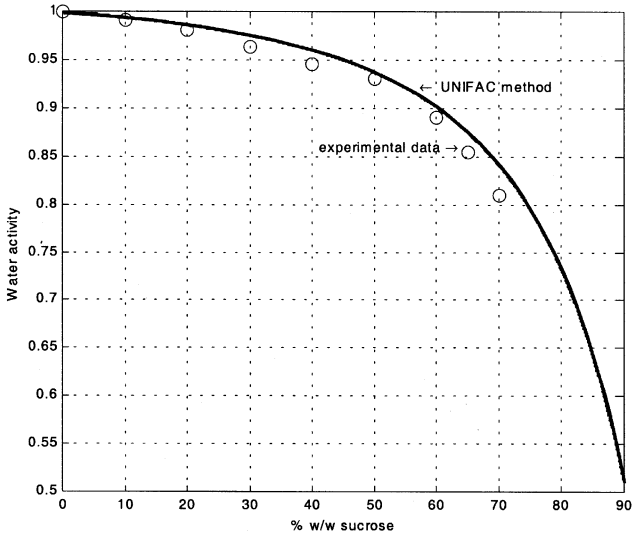

Figure 3. Water activity in a solution of sucrose at 298 K.

In Figures 2 and 3 the activity values calculated as described earlier are compared with the experimental data given by Courel (1999). We can observe that there is good agreement between the two sets of data.

Viscosity of sugar solutions

The viscosity of sweetened solutions such as fruit juices could vary widely due to the sugar content. This effect results in a net increase in the energy requirements due to a larger pressure drop through the membrane module. The diffusion coefficient value in the boundary layer, as well as the limitation attributed to the concentration polarization, will be directly related to the local level of solute concentration.

Equation 7 shows the sugar solution viscosity variation in the function of the temperature and sugar concentration (Courel, 1999).

$$\log \eta_{suc} = 22.46 x_{suc} - 3.114 + \frac{(30-(T-273))}{(91+(T-273))}\left(1.1+43.1 x_{suc}^{1.25}\right) \quad (7)$$

where η_{suc} is the dynamic viscosity in Pa·s, x_{suc} is the molar fraction of sucrose, and T is the temperature in K.

Figure 4 presents the evolution of the viscosity in the function of the sucrose concentration, which is estimated through Eq. 7 at two different temperatures.

Hydrodynamics

Courel (1999) obtained exceptionally high values of vapor water flow. Only Sheng (1993) reported comparable results for a laboratory-scale module (from 1.1×10^{-4} Kg·m·s to 2.2×10^{-3} kg·m^{-2}·s^{-1}), while other authors give fluxes below 1.1×10^{-3} kg·m^{-2}·s^{-1} for similar working conditions (Gostoli, 1999; Bailey et al., 2000; Gabelman and Hwang, 1999). In order to explain these results, it is necessary to take into account the particular design of the membrane module used by this author. This design is certainly responsible for

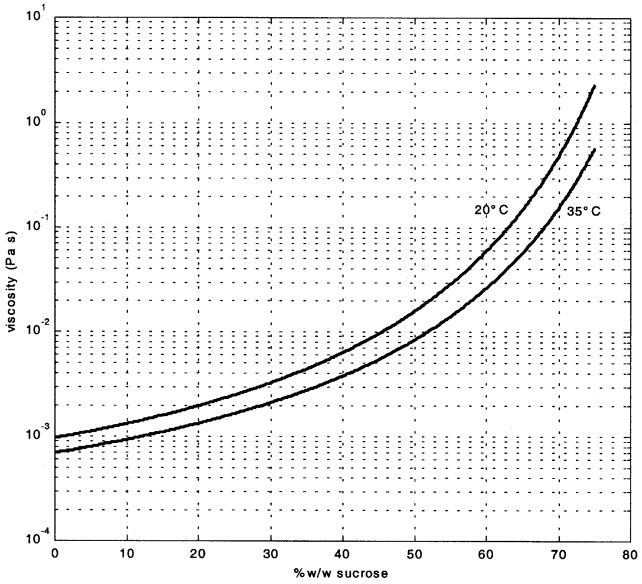

Figure 4. Viscosity of sucrose solution vs. solute concentration.

the complex hydrodynamic behavior, which is difficult to describe by means of a correlation as simple as the one initially selected to estimate the mass-transfer coefficients of Eqs. 1 and 5 (Mulder, 1996)

$$Sh = b_1 Re^{b_2} Sc^{b_3} \tag{8}$$

(a correlation by Calderbank and Young with: $b_1 = 0.082$, $b_2 = 0.69$, and $b_3 = 0.33$). Taking the assumption of a close analogy between momentum and mass-transport phenomena, Courel and coworkers (Courel et al., 2000b) proposed multiplying the mass-transfer coefficient values obtained with Eq. 8 by a correction factor corresponding to the ratio between measured and theoretical pressure drops in the membrane module.

The theoretical pressure drop is the one that would be obtained if the flow channel was straight according to

$$\Delta P^{th} = \frac{1}{2}\rho v^2 \frac{4f}{d_h} l \tag{9}$$

with

$$f = \frac{S}{1/2\,\rho v^2} \tag{10}$$

where ΔP^{th} is the theoretical pressure drop due to the wall friction, l is the total length of the tube, f is the dimensionless friction factor, and S is the shear stress on the wetted surface of the channel. For a turbulent liquid flow inside smooth circular tubes, the friction factor could be predicted from the Reynolds number by using the Blausius equation

$$f = 0.0791 Re^{-0.25} \tag{11}$$

The ratio between the experimental and theoretical pressure drops was found to be constant and equal to 9 ± 1 (Courel et al., 2000b) on both sides of the membrane (brine and sucrose solution). This result indicates that the presence of bends in the flow channel introduces a high level of turbulence in the circulating fluid even at moderate Reynolds values (between 150 and 1,500). Based on the assumption of a strict analogy between momentum and mass transfer, the liquid mass-transfer coefficients, $k^{\exp}$, could be obtained from the theoretical values provided by Eq. 8, k^{th}, as

$$\frac{k^{\exp}}{k^{th}} = \frac{\Delta P^{\exp}}{\Delta P^{th}} \tag{12}$$

This correction has been introduced in the model.

Heat transfer

The transfer in osmotic evaporation is always accompanied by heat transfer due to the phase changes on both sides of the membrane (water evaporation and condensation, respectively). In the experimental procedure chosen by Courel (2000a), the core temperatures of the two fluids are the same. Thus, the transfer of latent heat generates a temperature decrease on the solution side of the interface. On the other hand, there is a temperature increase on the brine side. These temperature polarization phenomena should be responsible for a decrease in the water-vapor flow through the membrane caused by the reduction in the process driving force, that is, a partial pressure difference across the hydrophobic layer.

In our previous article (Romero et al., 2003), we tried to quantify this phenomenon in terms of permeability reduction and transmembrane temperature profile. Under the working conditions chosen, it appears that the amplitude of the temperature variation remains below 2.5 K, leading to a water-vapor flow decrease of 16 to 24%.

In this work, we have chosen to introduce a correction of the estimate of mass-transfer coefficients to increase the simulation performance. This is, in fact, equivalent to recognizing that the importance of polarization (and particularly thermal effects) is less than that calculated and reported previously (Romero et al., 2003).

Because the experiments that are used as a basis for this new study were carried out under almost identical operating conditions (with the exception that a sucrose solution is used in place of pure water), we chose to ignore thermal polarization at the first approximation.

Numerical methods

To solve the system of equations (equations of mass and heat transfer, phase equilibrium, and evaluation of transport properties), a program has been written in Matlab (Mokhtari, 2000). As already stated, the system was considered under isothermal conditions, by neglecting the influence of temper-

ature polarization. The Regula Falsi algorithm (Quarteroni, 2000; Keryszig, 1991) was applied to reduce the number of iterations. In the program it is possible to modify all the operating variables, the type of the mass-transfer mechanisms (especially in the gas gap), and the structural parameters of the membrane.

The algorithm comprises several elementary cells that are associated with the different layers of the system, plus one specific cell for the introduction of structural parameters/operating conditions and other modules that generate the concentration values at the interfaces. The general program diagram was previously presented (Romero et al., 2003).

Results and discussion

As already indicated, water-flow values have been estimated in this work by taking a Knudsen-like diffusion into account. Generally, the algorithm allows an estimation of the water-flow values between 0.06 and 0.21 $mol \cdot m^{-2} \cdot s^{-1}$ (1×10^{-3} and 3.8×10^{-3} $kg \cdot m^{-2} \cdot s^{-1}$) when the sucrose concentration and the temperature vary between 0 and 50% w/w and 293 and 303 K, respectively, the brine concentration is 45% w/w of $CaCl_2$ and the circulation rate is 1.5 $m \cdot s^{-1}$ for the sucrose solution and 1.35 $m \cdot s^{-1}$ for the brine. Mass-transfer coefficients were estimated using Eqs. 8 and 12, while the thickness of the gas film was taken as 20 μm. It is worth recalling that in our previous work (Romero et al., 2003) we showed that the liquid penetration in the hydrophobic layer is noticeable, and could represent two-thirds of the membrane thickness given in Table 1. The transport through the rest of the hydrophobic layer was considered as diffusion in liquid phase. The simulation results and the experimental values published by Courel and coworkers (Courel et al., 2000a,b) are presented in Figure 5. The main variable studied is the sucrose concentration.

From Figure 5a, it is possible to observe that there is good agreement between the experimental and calculated data. The hydrodynamics and structural modifications introduced in the model improve the prediction of flow values considerably. Indeed, without considering these modifications, the estimated flows are at least 40% below the experimental values (Romero et al., 2003). The variation in flow as a function of solute concentration is correctly described. Simulations could be carried out only up to 50% w/w at the core, since beyond this value one approaches saturation conditions at the interface. Besides, solute crystallization occurs, and the functions

Table 1. Parameters Used for Simulation with Both TF200 and TF450 Membranes

Parameter	Value Considered
Hydrophobic layer	PTFE
r_{hl}	4.5×10^{-8} m
L_{hl}	6.0×10^{-5} m
ϵ_{hl}	0.8
τ_{hl}	1.1
Support	Polypropylene
L_s	10.5×10^{-5} m
ϵ_s	0.6
τ_s	1.1

Source: Courel (1999).

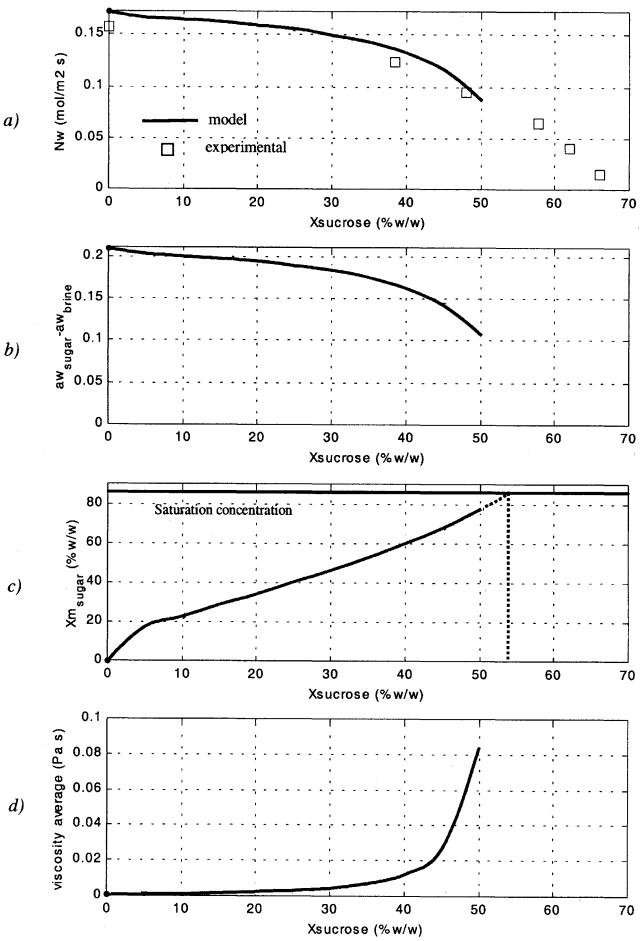

Figure 5. Variation in function of bulk sucrose concentration of (a) vapor water flow; (b) difference of activities at the hydrophobic layer interfaces; (c) sucrose concentration at the hydrophobic interface; (d) average viscosity of the solution to be treated.

used to estimate the thermodynamic and transport properties in the boundary layer do not work correctly. It should be noted that when the sucrose concentration varies between 0 and 50% w/w, the estimated value error remains lower than 9%.

Figure 5b clearly shows that the evolution of the difference in the activities at the interfaces is almost identical to the one recorded for water flow. In Figure 6 the linear relationship between different activities and the water flow through the membrane is emphasized. There is a new argument in favor of the thesis already defended in our previous work, according to which under our working conditions the mass-transfer resistance that controls the whole process corresponds to the gas gap trapped in the hydrophobic layer.

Figure 5c gives the values of the sucrose concentration at the interface with the hydrophobic layer vs. the bulk concentration. In spite of very favorable hydrodynamic conditions in the module channel, a net increase in the concentration in the boundary layer can be predicted. At a bulk concentration limit value between 52 and 53% w/w, the saturation of su-

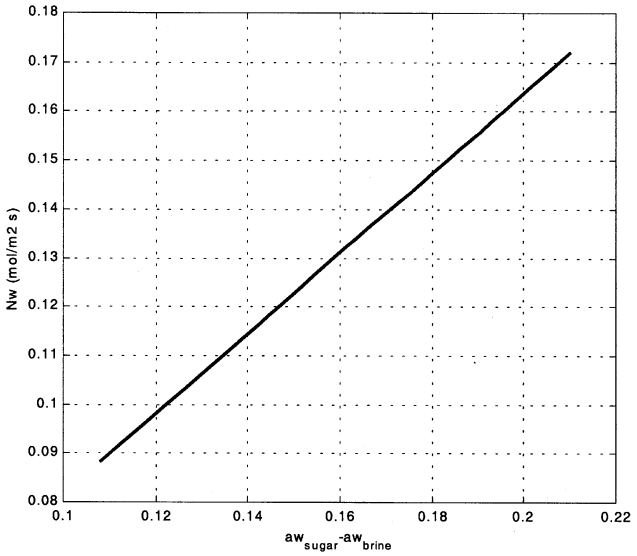

Figure 6. Water flow vs. difference of activities at interfaces.

crose, that is, about 86% w/w, is reached at the interface. This shows the main influence of concentration polarization in sucrose solutions.

Figure 5d confirms that the very rapid viscosity variation in the sugar concentration is responsible for the detrimental effects of polarization on performance. The average viscosity in the boundary layer can be 80 times higher than water viscosity. The gap is particularly noticeable when the OE process is used to concentrate solutions over 40% w/w.

Finally, Figure 7 shows the water flow evolution with sucrose concentration at different temperatures (between 293 K and 303 K). The water flow remains very close to those measured by Courel (2000a,b). This result attests to the robustness of the model developed here.

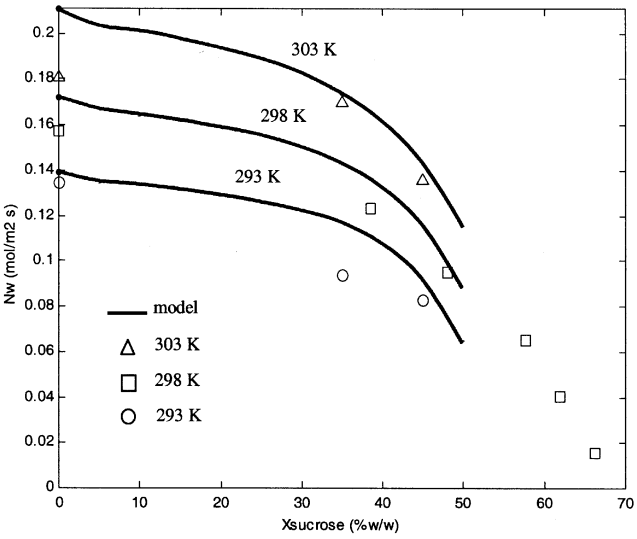

Figure 7. Water flow vs. bulk sucrose concentration and temperature.

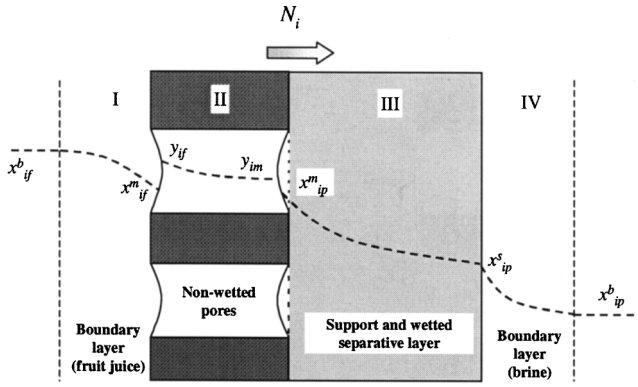

Figure 8. The concentration profile of the aroma compound *i*.

Transport of Volatile Organic Compounds

Theoretical approach

If several volatile organic compounds (VOCs) are present, their mutual interactions could be neglected, since their concentrations could be considered very low. In what follows we focus on just one of them, hereinafter referred to as the *i*-compound.

Through the boundary layer due to the sugar concentration on the solution side, the total flux of a particular aroma compound, i, can be written as a function of the bulk and interface concentration difference

$$N_i = k_i^{(\mathrm{I})}\left(x_{if}^b - x_{if}^m\right) \tag{13}$$

where $k_i^{(\mathrm{I})}$ can be estimated using an appropriate mass-transfer correlation.

An expression based on the activity coefficient, γ_{if}, can be used to calculate the vapor–liquid equilibrium at the membrane interface

$$x_{if}^m \gamma_{if} P_i^{\mathrm{sat}} = y_{if} P \tag{14}$$

with P_i^{sat} the vapor pressure of i at saturation, and P is the absolute gas pressure. It is worth noting that $\gamma_{if} P_i^{\mathrm{sat}}$ represents the Henry constant.

The mass transfer of volatile compounds through the membrane can be described by Eq. 15, where the total flux of compound i is given by two terms. The first term on the righthand side represents the diffusion contribution within the pore; in this case, the driving force is the gradient of the partial pressure of component i. The second term is the contribution due to total mass flux (aroma and water) through the membrane (Bird et al., 1982). This last term corresponds to the aroma driven by water vapor (ADWV), as in steam distillation processes

$$N_i = J_i + y_i \sum_{j=1}^{n} N_j \tag{15}$$

Table 2. Composition of the Model Solutions

Compound	Initial Concentrations Initial Sucrose Concentration	
	15 brix	35 brix
Sucrose	15.0% w/w	35% w/w
Citric acid	3.7% w/w	7.4% w/w
Benzaldehyde	5.0 $mg \cdot kg^{-1}$	5.0 $mg \cdot kg^{-1}$
Hexanol	5.0 $mg \cdot kg^{-1}$	5.0 $mg \cdot kg^{-1}$
Ethyl butanoate	5.0 $mg \cdot kg^{-1}$	5.0 $mg \cdot kg^{-1}$
Hexyl acetate	5.0 $mg \cdot kg^{-1}$	5.0 $mg \cdot kg^{-1}$

Source: Courel (1999).

In our case, considering that within the pore only water vapor, air, and the aroma compound i are present, it becomes

$$N_i = J_{i,\text{gas}} + y_i(N_i + N_w + N_a) \tag{16}$$

Considering that the aroma compounds present a molecular weight higher than water, $J_{i,\text{gas}}$ has been described using molecular diffusion. We shall see later that the conclusions at which one arrives while making the assumption of a Knudsen transport mechanism are identical from a qualitative point of view. Because the transport of air through the interfaces is negligible ($N_a = 0$), the total flux is given by

$$N_i(1 - y_i) = \frac{\epsilon_{hl}}{\tau_{hl}} C_{\text{gas}} D_{i,\text{gas}} \frac{dy_i}{dz} + y_i N_w \tag{17}$$

where C_{gas} is the total molar concentration, $D_{i,\text{gas}}$ is the diffusion coefficient of the i-compound in the gas mixture within the pores, and y_i is the molar fraction of i in the gas phase.

Integrating Eq. 17 with the boundary conditions $z = 0 \rightarrow y_i = y_{if}$ and $z = L_{\text{gas}} \rightarrow y_i = y_{im}$, where L_{gas} is the membrane thickness, Eq. 18 follows

$$\int_0^{L_{\text{gas}}} N_i \, dz = \frac{\epsilon_{hl}}{\tau_{hl}} \int_{y_{if}}^{y_{im}} C_{\text{gas}} D_{i,\text{gas}} \frac{dy_i}{1 - y_i} + \int_0^{L_{\text{gas}}} N_w \frac{y_i}{1 - y_i} dz \tag{18}$$

At steady state, because the values of concentration y_i are weak, the following expression of the process selectivity results by integrating vs. z

$$\frac{N_i}{N_w} = \Omega \frac{y_{if} - y_{im}}{N_w} + \overline{y_i} \tag{19}$$

where $\overline{y_i}$ represents the mean values of y_i in the gas gap.

As already indicated, we can note that the same kind of expression also should be obtained under the assumption of a Knudsen diffusion. Simply put, the expression of Ω—a function of the membrane structural characteristics, the aroma diffusivity, and the total gas pressure—would be modified.

Two additional resistances due to the liquid trapped within the porous structure and the boundary layer on the brine side should be considered. They could be described by Eqs. 20 and 21

$$N_i = J_{i,\text{brine}} + x_i(N_i + N_w + N_{\text{salt}}) \tag{20}$$

$$N_i = k_i^{(\text{IV})}\left(x_{ip}^x - x_{ip}^b\right) \tag{21}$$

by an analogy, which has already been made with Eqs. 16 and 13, respectively. Because the main resistance is due to the boundary layer in the sweetened solution and the gas gap, further analysis has been limited to their effects.

Results and discussions

Thermal effects. According to Eq. 17, thermal effects that have been neglected as a first approximation in this study could affect the transport of the aroma compound in two ways: by decreasing the diffusion contribution due to the variation of the partial pressure gradient, and by lowering the term that corresponds with the ADWV due to the drop of N_w. A complete simulation well beyond the scope of this work should help to specify these variations.

Vapor–Liquid Equilibrium. Another very important point concerning the mass transfer of volatile compounds, and, thus, the process selectivity, is the vapor–liquid equilibrium. There is only a limited number of studies on the composition and VLE of fruit juices. A complete description of the composition of passion fruit juice has been carried out by Casimir and coworkers (1981). The specific compounds selected by Courel (1999) to constitute the model solution (see Table 2) occur among the three main chemical groups of aroma compounds: esters, alcohols, and aldehydes.

Equilibrium data deduced from experiments have been presented by several authors (Massaldi and King, 1973; Kieckbusch and King, 1979; Carelli et al., 1991; Sancho et al., 1997). Predictive methods (for example, UNIFAC and ASOG) are also mentioned in the literature (Zhang et al., 2002; Brendel and Sandler, 1999). Some values of activity coefficients at infinite dilution for the compounds used by Courel (1999) are presented in Table 3; the values of Antoine constants that are given in Table 4 allow the estimation of the vapor pressure at saturation for two of them.

Massaldi and King (1973) emphasized the increase in the value of the activity coefficient of the hexyl acetate in the

Table 3. Values of Activity Coefficients at Infinite Dilution of Some Aroma Compounds

Compound	γ^∞	Conditions
Benzaldehyde	559–593	50–68°C, model solutions (Carelli et al., 1991)
	963	25°C, water (Sancho et al., 1997)
Hexanol	866–1,047	41–64°C; model solutions (Carelli et al., 1991)
Hexyl acetate	15,000–22,000	25°C; 0–60% w/w sucrose (Massaldi and King, 1973)

Table 4. Antoine Constants of Some Aroma Compounds (Carelli et al., 1991)

	Ln P^s (kPa) = $A - B/(C + T(K))$			
Compound	A	B	C	T range, K
Benzaldehyde	14.3351	3748.62	−66.12	300–460
Hexanol	16.0848	4055.45	−76.49	308–430

Source: Carelli et al. (1991).

function of the sucrose concentration. This fact could explain the improvement in the flux value measured by Courel (1999) when the sugar concentration is more elevated (see Table 5). In addition Brendel and Sandler (1999) have studied the VLE of volatile organic compounds in brines: their results show an improvement of the activity coefficient values at infinite dilution as a function of NaCl concentration. Such a modification of the VLE of volatile compounds in the presence of a salt should minimize the loss of aroma compounds in OE by decreasing the diffusion contribution within the gas layer.

The main obstacle to application of the models and their intensive use for simulation is today the lack of reliable thermodynamic data. For this reason, we limited our work in what follows to show the global tendencies of the system, by only comparing, in a specific way, the predictions with the experimental points provided by Courel (1999).

Mass-Transfer Considerations. Courel (1999) has studied the mass transfer of aroma compounds in a model solution. This model for simulating the behavior of a particular tropical fruit, the passion fruit (*P. edulis*), includes four representative aroma compounds, and citric acid, which is another important solute as regards the quality. Investigations were carried out with various amounts of sucrose, found at different intermediate steps of the process. The decrease in the water content of the model solution was determined by refractometric measurements, and the evolution of the content of the aroma compounds was followed by gas chromatography. From these measurements, the values of flux at steady state have been estimated. Results are shown in Table 5.

In our previous studies, it has been shown that the water transfer in the OE process is mainly controlled by the driving force through the gas layer, that is, the difference in the partial pressure of water vapor that does not exceed 1,000 Pa in the classic conditions. This assumption remains valid for fruit juices, considering that water represents more than 95% of their composition. Equation 17 indicates that there are two terms that participate in the total flux of volatile compounds: the first term related to the diffusive contribution, and the second term is related to the contribution given by the total

Table 5. Experimental Mean Values of Flux of Volatiles Compounds at Steady State

	N (mol·m^{-2}·s^{-1}) Initial Sucrose Concentration	
Compound	15 brix	35 brix
Benzaldehyde	8.31×10^{-9}	6.75×10^{-9}
Hexanol	6.26×10^{-9}	6.60×10^{-9}
Ethyl butanoate	6.23×10^{-9}	6.69×10^{-9}
Hexyl acetate	0.55×10^{-9}	1.69×10^{-9}
Water	7.72×10^{-3}	8.21×10^{-3}

Source: Courel (1999).

Table 6. Experimental and Estimated Values of Selectivity (N_i/N_w) of Aroma Compounds in Fruit Juice Concentration by OE Process

	(N_i/N_w)	
Compound	Experimental (Courel, 1999)	Estimated by Eq. 10
Benzaldehyde	1.08×10^{-6}	9.30×10^{-7}
Hexanol	8.11×10^{-7}	1.08×10^{-6}

mass transfer. Under certain conditions, and especially for high values of N_w, which is the case with the absolute values of flux found by Courel (1999), this second term could represent the major contribution to the flux of volatile compounds. We can observe that the experimental data obtained by Courel (1999) (see Table 5) move well in this direction: with the exception of benzaldehyde, the flux values of aroma compounds increase with water flux. The strong increase of the activity-coefficient value for hexyl acetate vs. sucrose concentration, already emphasized (Massaldi and King, 1973), could be responsible for the net increase in organic flux observed with this compound between 15 and 35 Brix.

Another main argument in favor of this hypothesis is that, by using Eq. 19 and making the assumption that the second term on the right side is predominant if the polarization phenomenon at the boundary layer is not very important, it is possible to calculate selectivity values for aroma compounds as $N_i/N_w \cong \overline{y_i}$. The estimated values are very close to experimental values as indicated in Table 6. On the contrary, in the absence of this assumption, the error between the calculated and measured values remains very important.

From a general point of view, and according to Eq. 20, there should be two distinct regimes:

1. One for which the first term on the right side would be important: in that case, water flux is low and mass transfer is controlled by diffusion; to increase selectivity the main focus would be to decrease Ω (through the choice of membrane characteristics) and/or to increase the water flux; this could be done by lowering the detrimental effect of the boundary layer on the sugar solution side (good hydrodynamic conditions and high tangential velocity);
2. One for which the second term would represent the major part: in that case, water flow is high and mass transfer is controlled by convection; to increase selectivity, the main focus would be to decrease $\overline{y_i}$, by enhancing the importance of the polarization layer on the sucrose solution side, that is, by circulating this solution along the membrane at a low velocity; this conclusion is contrary to the one made for the previous regime.

As a whole, the final choice for the design and working conditions of the process should be made by taking into account these arguments concerning the selectivity (N_i/N_w), and also considering the constraints on productivity (N_w).

Note that the opposite conclusions should be adopted in the case where the process for achieving the main objective would be to extract and not reject volatile compounds.

Conclusions

The simulation results presented in this work make it possible to thoroughly explain the behavior of experimental wa-

ter flux and to quantify the effect of concentration polarization in the OE process when a sugar solution is concentrated.

The mass-transfer resistance that mainly controls the process is located in the gas layer that fills the porosity of the hydrophobic membrane; however, the concentration polarization that develops on the sucrose side at elevated solute contents can also significantly influence the final performance. Indeed, it is responsible not only for a steep increase in the fluid viscosity but it also affects the water activity at the interface, thus decreasing the driving force through the hydrophobic layer: the difference in the partial pressure of water vapor remains below 1,000 Pa in the classic conditions studied. The influence of the temperature on the driving force was also demonstrated.

In this work two major modifications were introduced, in comparison to the initial model presented by our group (Romero et al., 2003). The first lies in a more appropriate hydrodynamic characterization of the membrane module; the second relates to the importance of gas layer mass-transfer resistance, which could be modified by the depth of liquid penetration within the hydrophobic layer. It is clearly established that these corrections considerably improve the accuracy of the model. In another geometry system, they could be modified following the same methodology presented here.

The proposed work also attempts to understand the possible transport mechanisms of the aroma compounds for the fruits juices concentration in the OE process. These mechanisms depend on the operating conditions, structural parameters, and thermodynamic considerations of the solutions.

Mainly, the model presented in this work indicates that there are two terms that participate in the total flux of the volatile compounds: the diffusive contribution due to the gradient of the partial pressure within the pores, and the contribution given by total mass transfer (ADWV) through the membrane. From the equations, it is possible to estimate selectivity. The values obtained assuming the major ADWV contribution is very close to the experimental values presented by Courel (1999).

From a general point of view, there should be two distinct regimes: one for which the diffusion contribution would be predominant; in that case, the water flux would be low and selectivity would depend on the membrane characteristics and/or favorable hydrodynamic conditions. One for which the ADWV contribution represents the major part; in this case, the water flow would be high and the mass transfer would be controlled by convection; to increase selectivity, the major focus would be on decreasing the partial pressure in the gas and/or increasing the importance of the polarization layer.

Following the general schema provided by Romero et al. in their first paper (2003), the results should be improved by accounting for thermal polarization while agreeing to definitely make the computational times longer.

Acknowledgments

The financial support of the University of Santiago de Chile and the French Government for Julio Romero's Ph.D. studies is gratefully acknowledged.

Notation

b_1 = constant in Eq. 8
b_2 = constant in Eq. 8
b_3 = constant in Eq. 8
C = total molar concentration, $mol \cdot m^{-3}$
d = dia., m
D = diffusion coefficient, $m^2 \cdot s^{-1}$
f = corrected friction factor
G = permeance, $mol \cdot m^{-2} \cdot s^{-1} \cdot Pa^{-1}$
k = mass-transfer coefficient, $mol \cdot s^{-2} \cdot s^{-1}$
L = thickness, m
l = length of the tube, m
M = molecular weight, $kg \cdot mol^{-1}$
N = mass flow, $mol \cdot m^{-2} \cdot s^{-1}$
P = pressure in the pore of the hydrophobic membrane, Pa
p = partial pressure, Pa
R = gas constant, $J \cdot mol^{-1} \cdot K^{-1}$
r = pore radius, m
Re = Reynolds number
S = shear stress, Pa
Sc = Schmidt number
Sh = Sherwood number
T = temperature, K
v = circulation rate of solution, $m \cdot s^{-1}$
x = molar fraction in liquid phase
y = molar fraction in gas phase
z = coordinate z

Greek letters

γ = activity coefficient
γ^{∞} = activity coefficient at infinite dilution
ΔP = pressure drop, Pa
ϵ = porosity
η = viscosity, $Pa \cdot s$
ρ = density, $kg \cdot m^{-3}$
τ = tortuosity
Ω = diffusion factor defined in Eq. 20, $mol \cdot m^{-2} \cdot s^{-1}$

Subscripts and superscripts

a = air
b = bulk conditions
$brine$ = brine
$CaCl_2$ = calcium solution
f = feed solution
gas = gas phase within the pores
h = hydraulic
hl = hydrophobic layer
i = i-component
Kn = Knudsen regime
MD = molecular diffusion regime
p = permeate side
s = support property
$salt$ = salt of the extraction solution
suc = sucrose
w = water
(I) = boundary layer in the feed solution
(II) = within the pores of hydrophobic layer
(III) = within the pores of the support
(IV) = boundary layer of the brine
b = bulk conditions
C = combinatorial
$D\text{-}H$ = Debye-Hückel
exp = experimental
m = in contact with the gas layer
R = residual
s = in contact with the support
sat = saturation condition
sup = at average conditions within the support
th = theoretical

Literature Cited

Achard, C., J. B. Gros, and C. G. Dussap, "Prédiction de l'Activité de l'Eau, des Températures d'Ébullition et de Congélation de Solutions Aqueuses de Sucres par un Modèle UNIFAC," *Cah. Sci.*, **109**, 93 (1992).

Bailey, A. F. G., A. M. Barbe, P. A. Hogan, R. A. Johnson, and J. Sheng, "The Effect of the Ultrafiltration on the Subsequent Concentration of Grape Juice by Osmotic Distillation," *J. Membr. Sci.*, **164**, 195 (2000).

Bandini, S., and G. C. Sarti, "Concentration of Must Through Vacuum Membrane Distillation," *Desalination*, **149**, 253 (2002).

Baudot, A., I. Souchon, and M. Marin, "Total Permeate Pressure Influence on the Selectivity of the Pervaporation of Aroma Compounds," *J. Membr. Sci.*, **158**, 167 (1999).

Bird, R. B., W. E. Stewart, and E. N. Lightfoot, *Fenómenos de Transporte*, Reverté, Barcelona, Spain (1982).

Börjesson, J., H. O. E. Karlsson, and G. Trägårdh, "Pervaporation of a Model Apple Juice Aroma Solution: Comparison of Membrane Performance," *J. Membr. Sci.*, **119**, 229 (1996).

Brendel, M. L., and S. I. Sandler, "The Effect of Salt and Temperature on the Infinite Dilution Activity Coefficients of Volatile Organic Chemicals in Water," *Fluid Phase Equilib.*, **165**, 87 (1999).

Carelli, A. A., G. H. Crapiste, and J. E. Lozano, "Activity Coefficients of Aroma Compounds in Model Solutions Simulating Apple Juice," *J. Agric. Food Chem.*, **39**, 1636 (1991).

Casimir, D. J., J. F. Kefford, and F. B. Whitfield, "Technology and Flavor Chemistry of Passion Fruit Juices and Concentrates," *Advances in Food Research*, Vol. 27, Chichester and Stewart, eds., Academic Press, New York, p. 243 (1981).

Correa, A., J. F. Comesaña, J. M. Correa, and A. M. Sereno, "Measurement and Prediction of Water Activity in Electrolyte Solutions by a Modified ASOG Group Contribution Method," *Fluid Phase Equilibria*, **129**, 267 (1997).

Couffin, N., C. Cabassud, and V. Lahoussine-Turcaud, "A New Process to Remove Halogenated VOCs for Drinking Water Production: Vacuum Membrane Distillation," *Desalination*, **177**, 233 (1998).

Courel, M., *Etude des Transferts de Matiére en Évaporation Osmotique: Application à la Concentration des Jus de Fruits*, PhD Thesis, Univ. of Montpeller II, Montpellier, France (1999).

Courel, M., M. Dornier, J. M. Herry, G. M. Rios, and M. Reynes, "Effect of Operating Conditions on Water Transport During the Concentration of Sucrose Solutions by Osmotic Distillation," *J. Membr. Sci.*, **170**, 281 (2000a).

Courel, M., M. Dornier, G. M. Rios, and M. Reynes, "Modelling of Water Transport in Osmotic Distillation Using Asymetric Membrane," *J. Membr. Sci.*, **173**, 107 (2000b).

Gabelman, A., and S. Hwang, "Hollow Fiber Membranes Contactors," *J. Membr. Sci.*, **159**, 61 (1999).

Gostoli, C., "Thermal Effects in Osmotic Distillation," *J. Membr. Sci.*, **163**, 75 (1999).

Kreyszig, E., *Matemáticas Avanzadas Para Ingeniería*, Limusa-Noriega, ed., México City, Mexico (1991).

Kiechkbusch, T. G., and J. King, "Partition Coefficients for Acetate in Food Systems," *Agric. Food Chem.*, **3**, 504 (1979).

Massaldi, H. A., and J. King, "Simple Technique to Determine Solubilities of Sparingly Soluble Organics: Solubility and Activity Coefficients of *d*-Limonene, *n*-Butylbenzene, and *n*-Hexyl Acetate in Water and Sucrose Solutions," *J. Chem. Eng. Data*, **4**, 393 (1973).

Mokhtari, M., *Matlab* 5.2 & 5.3 *et Simulink* 2 & 3 *pour Étudiants et Ingénieurs*, Springer-Verlag, Berlin (2000).

Mulder, M., *Basic Principles of Membrane Technology*, Kluwer, Dordrecht, The Netherlands (1996).

Quarteroni, A., *Méthodes Numériques pour le Calcul Scientifique*, Springer-Verlag, Paris (2000).

Romero, J., G. M. Rios, J. Sanchez, S. Bocquet, and A. Saavedra, "Modeling heat and mass transfer in osmotic evaporation process," *AIChE J.*, **49**(2), 300 (2003).

Romero, J., G. M. Rios, J. Sanchez, and A. Saavedra, "Modelling and Simulation of Osmotic Evaporation Process," *Proc. Conf. on Engineering with Membranes*, Vol. II, Granada, Spain, p. 297 (2001).

Sancho, M. F., M. A. Rao, and D. L. Downing, "Infinite Dilution Activity Coefficients of Apple Juice Aroma Compounds," *J. Food Eng.*, **34**, 145 (1997).

Shaban, H., "Removal of Water from Aroma Aqueous Mixtures Using Pervaporation Processes," *Sep. Technol.*, **6**, 69 (1996).

Sheng, J., "Osmotic Distillation Technology and Its Applications," *Aust. Chem. Eng. Conf.*, **3**, 429 (1993).

Zhang, S., T. Hiaki, and K. Kojima, "Prediction of Infinite Dilution Activity Coefficient for Systems Including Water Based on the Group Contribution Model with Mixture-Type Groups. II Extension and Applications," *Fluid Phase Equilib.*, **198**, 15 (2002).

Manuscript received Dec. 16, 2002, and revision received Mar. 28, 2003.